SAND2000-0441J

Factors controlling satiated relative permeability in a partially-saturated horizontal fracture

M.J. Nicholl

School of Geology, Oklahoma State University, Stillwater

H. Rajaram

Department of Civil, Environmental, and Architectural Engineering, University of Colorado, Boulder

R.J. Glass

Flow Visualization and Processes Laboratory, Sandia National Laboratories, Albuquerque, New Mexico

Abstract. Recent work demonstrates that phase displacements within horizontal fractures large with respect to the spatial correlation length of the aperture field lead to a *satiated* condition that constrains the relative permeability to be less than one. We use effective media theory to develop a conceptual model for *satiated relative permeability*, then compare predictions to existing experimental measurements, and numerical solutions of the Reynolds equation on the measured aperture field within the flowing phase. The close agreement among all results and data show that for the experiments considered here, in-plane tortuosity induced by the entrapped phase is the dominant factor controlling satiated relative permeability. We also find that for this data set, each factor in the conceptual model displays an approximate power law dependence on the satiated saturation of the fracture.

Introduction

The permeability of a fracture to a given fluid phase is determined by the geometry of that phase, which in turn evolves during the displacement of one fluid (defending phase) by another (invading phase). At any given stage of its development, phase geometry is a history dependent product of competition between local capillary, viscous, and gravity forces [Glass et al., 1995]. In a statistically homogeneous horizontal fracture much larger than the spatial correlation length of the aperture field, slow steady displacement along the plane of the fracture leads to a *satiated* condition where the invading phase spans the fracture in all directions, and the remaining defending phase is fully entrapped [Glass et al., 1998].

Following invasion to a satiated state, lack of an escape path for the entrapped defending phase precludes further changes in the geometry of the respective phases (flowing invader and entrapped defender), unless: 1) the entrapped phase is dislodged by viscous forces, or dissolved into the flowing phase; 2) a change in boundary conditions reverses the roles of invader and defender; or 3) aperture variability leads to repeated fragmentation of the phase structure. Because the permeability of a horizontal fracture under satiated conditions can be reduced by over 80% from its fully saturated value [Nicholl and Glass, 1994], and because horizontal fractures are ubiquitous in nature, development of a constitutive relation for *satiated relative permeability* is critical for modeling flow in partially-saturated fractured rock.

Here we present a simple conceptual model for satiated relative permeability which explicitly considers several factors that act to reduce fracture permeability under partially-saturated conditions. Existing experiments [Nicholl and Glass, 1994] provide data to evaluate the conceptual model, and implement numerical simulations that employ the Reynolds equation to model flow on measured aperture and phase geometries. We demonstrate the relative importance of the various factors in the conceptual model, and find empirically that each exhibits an approximate power law dependence on saturation.

Conceptual model

Following the porous media literature, we employ relative permeability (k_r) as a measure of the reduction in permeability to a given phase that occurs between partially (k_f), and fully saturated (k) conditions; i.e., $k_r = k_f/k$. Here, we are interested in the satiated value of the relative permeability (k_{rs}) that limits the maximum value of k_r to be less than one. Zimmerman and Bodvarsson [1996] suggested that in a variable conductivity field, predictions of flow obtained through an effective medium approach [e.g., Landau and Lifshitz, 1960] could be combined with corrections derived for flow around obstructions in a Hele-Shaw cell. This approach assumes negligible drag along the edges of the obstructions (free-slip boundary), extension to satiated fracture flow also requires that the immobile entrapped phase locally fills the aperture (figure 1). Recasting their results in terms of steady volumetric flow (Q) through a saturated fracture of width (W) under a constant hydraulic gradient (i) yields the following relation:

$$Q = \left[\frac{\langle b\rangle^3 g}{12\nu}\left(1+\frac{9\sigma_b^2}{\langle b\rangle^2}\right)^{-1/2}\right] W i \qquad (1)$$

where ν is the kinematic viscosity, g is the acceleration due to gravity, $\langle b\rangle$ and σ_b^2 are respectively the mean and variance of the aperture field.

Lateral diversion of flow by an immobile entrapped phase increases average path length through the fracture with respect to that for the saturated case. This acts to decrease the effective hydraulic gradient, and consequently fracture permeability. A tortuosity factor (t) is employed to represent the decrease in permeability resulting from in-plane tortuosity induced by the entrapped phase. Under these conditions we have:

$$Q_f = \left[\frac{\langle b_f\rangle^3 g}{12\nu}\left(1+\frac{9\sigma_{b_f}^2}{\langle b_f\rangle^2}\right)^{-1/2}\right] \langle W_f\rangle \tau i \qquad (2)$$

where the subscript (f) refers to parameters ($\langle b\rangle$, σ_b^2, and $\langle W\rangle$) for the region occupied by the flowing phase. The product of $\langle W_f\rangle$ and t corresponds to correction terms for contact area presented by Zimmerman and Bodvarsson [1996]. As discussed in their work, the

DISCLAIMER

DISCLAIMER

Portions of this document may be illegible in electronic image products. Images are produced from the best available original document.

correction terms can be evaluated explicitly for simple entrapped phase geometries (e.g., widely separated circular features).

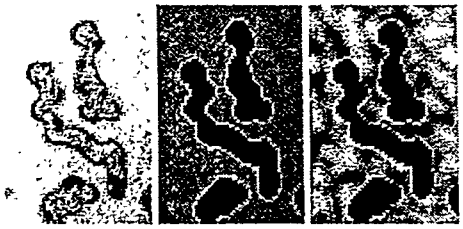

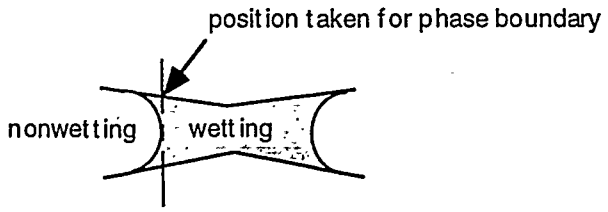

Figure 1. Phase geometry. Raw data (a) shows entrapped phase clusters (dark gray) surrounded by the flowing phase (light gray). The dark band separating the two phases results from refraction of light at the curved fluid-fluid interface (b). Width of this band will be ~b/2 (~0.01 cm), which is close to our pixel size (0.0143 cm) The algorithm developed for this work defined the boundary between phases at the outside edge of the trapped region; i.e., outside edge of the dark band. We note that use of discrete data (image pixels) induces some uncertainty regarding the interface location. Definition of the interface is then used to produce a field (c) for tortuosity calculations in which the flowing phase is given by b = 1, and the entrapped phase by b = 0. Multiplication of (c) by the aperture field, b(x,y), provides geometry of the flowing phase (d) which is used to determine statistical measures, and for numerical simulations applying the Reynolds equation to the variable aperture field.

For flow through a cross-sectional area given by the product of W and ⟨b⟩, Darcy's law gives:

$$Q = \frac{kg}{\nu}\langle b\rangle W i \qquad (3)$$

Thus, k and k_f may be obtained from (1) and (2) respectively, using (3). The ratio $k_{rs} = k_f/k$ is then obtained as:

$$k_{rs} = S_f \tau \underbrace{\left[\frac{\langle b_f\rangle^2}{\langle b\rangle^2}\right]}_{A}\underbrace{\left[\left(1+\frac{9\sigma_b^2}{\langle b\rangle^2}\right)^{1/2}\left(1+\frac{9\sigma_{b_f}^2}{\langle b_f\rangle^2}\right)^{-1/2}\right]}_{B} \qquad (4)$$

where saturation of the flowing phase (S_f) describes the average fraction of the cross-sectional area that participates in flow, and is given by: $S_f = (\langle W_f\rangle\langle b_f\rangle)/(W\langle b\rangle)$.

Four major contributors to fracture relative permeability are identified in (4): saturation (S_f), tortuosity factor (τ) accounting for in-plane tortuosity induced by the entrapped phase, mean aperture within the flowing phase (part A), and the distribution of apertures within the flowing phase (part B). Each of these factors describes a modification to the geometry of the flowing phase by an immobile entrapped phase that fully spans the local aperture. With the exception of the tortuosity factor (τ), which is difficult to measure directly, the terms on the right-hand-side of (4) can be obtained from measurements of aperture and phase geometry.

Experimental data

Several experiments considering steady flow of water in a horizontal analog fracture were presented by Nicholl and Glass [1994]. Permeability was measured for the saturated case (k), and seven satiated cases (k_{rs}). The size of their homogeneous, isotropic fracture (~15 x 30 cm) was much larger than the correlation scale (0.08 cm) of the aperture field; the entrapped phase imposed flow structure at, or above, the aperture correlation scale. Each of their experiments considered a different spatial distribution of the wetting (water) and nonwetting (air) phases within the fixed aperture field b(x,y), ($\langle b\rangle$ = 0.023 cm, σ_b = 0.0062 cm). The phase geometries were designed to represent a variety of invasion histories, and as a result differ vastly between trials (see figure 2), as does the saturation at satiation (table 1). Invasion processes reflected: redistribution of the air phase within a partially-saturated fracture through imposition of significant viscous forces (experiments rp2, rp4); rapid drainage from saturation (S_f = 1), followed by slow reinvasion of water (rp1, rp3); and slow nonwetting phase invasion of a saturated fracture, followed by slow reinvasion of water (rp5-7). Transmitted light imaging was used to measure aperture, and identify the phase occupying each pixel at 0.0143 cm resolution over a 12.3 x 27.9 cm section of the fracture (855 x 1950 grid points); ~1 cm along the fracture edges was obscured by the apparatus. Here, we refined their original aperture field measurements using data analysis techniques presented by Detwiler et al. [1999]. We also developed improved algorithms for locating the boundaries separating the air and water phases (see figure 1). Further details of the experiments, as well as images of all phase structures considered here can be found in Nicholl and Glass [1994].

Table 1. Summary of data and results

	S_f	$\langle b_f\rangle$ (cm)	σ_{bf} (cm)	equation (4) part B	equation (4) part A	τ	k_{rs} eq. (4)	k_{rs} simulated[1]	k_{rs} experiment	$S^{3.4}$
rp0[2]	1.00	0.023	0.0062							
rp1	0.47	0.020	0.0057	0.97	0.75	0.36	0.12	0.12	0.11	0.078
rp2	0.86	0.022	0.0062	0.99	0.95	0.81	0.66	0.75	0.73	0.61
rp3	0.54	0.020	0.0059	0.97	0.79	0.40	0.16	0.16	0.15	0012
rp4	0.94	0.022	0.0062	1.00	0.98	0.94	0.87	0.91	0.90	0.82
rp5	0.62	0.021	0.0061	0.97	0.85	0.41	0.21	0.20	0.20	0.19
rp6	0.59	0.020	0.0059	0.98	0.82	0.30	0.14	0.13	0.15	0.16
rp7	0.62	0.021	0.0060	0.98	0.84	0.33	0.17	0.17	0.16	0.20

[1]simulated on variable aperture field, b(x,y)

[2]saturated case (aperture field)

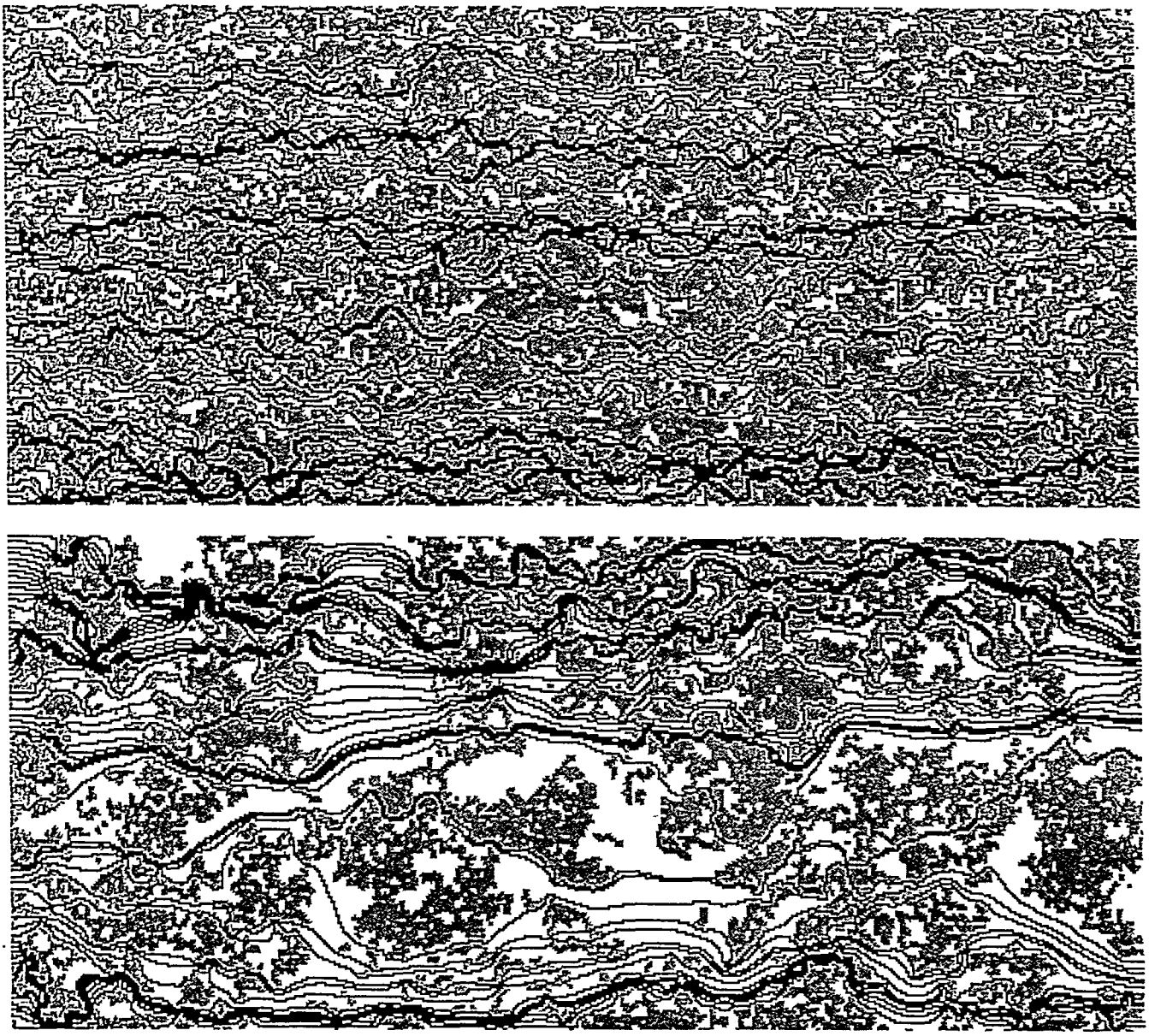

Figure 2. Example phase structures showing streamlines. Flowing phase (white) surrounds the immobile entrapped phase (gray). Streamlines (black) were produced by advective particle tracking on simulated pressure fields. The upper image (rp1) shows numerous channels moving through a field consisting of relatively small, but densely packed clusters of the entrapped phase ($S_f = 0.47$, $k_r = 0.11$). Tortuosity exhibits a principal wavelength on a scale similar to that of the entrapped phase clusters. Phase geometry in the lower image (rp7) concentrates flow into a smaller number of channels ($S_f = 0.62$, $k_r = 0.16$). The large entrapped phase clusters induce long-wavelength tortuosity and create significant "dead zones" which are bypassed by flow. Other phase structures analyzed in this paper are described in Nicholl and Glass [1994].

Results and discussion

Nicholl and Glass [1994] calculated τ from their experimental data by assuming that $k_{rn} = S_f\tau\langle b_f\rangle^2/\langle b\rangle^2$. Here, we obtain an independent estimate of τ by simulating flow on their measured phase geometries in the absence of aperture variability (i.e., $b = 1$ for the flowing phase, $b = 0$ for the trapped phase). In this case, (4) reduces to $k_{rn} = S_f\tau$. Dividing simulated flow rate in the presence of an entrapped phase by that obtained for the saturated case gives k_{rn}; S_f is taken from the measured phase structure, leaving τ.

We also performed simulations that included aperture variability, b(x,y), within the flowing phase. For both cases, we used a finite-difference implementation of the Reynolds equation on a 855 x 1950 grid. Link transmissivities (irrelevant for the $b = 1$ case) were taken to be the harmonic average of adjacent values; additional details on the numerical method are provided in Nicholl et al. [1999]. Predictions based on (4), and simulations on the variable aperture field (table 1) both closely reproduce experimental estimates of k_{rn}, predicting 90-99% of the measured decrease in permeability from saturated to satiated conditions.

The discrepancies between predictions and experimental measurements of k_{rn} can be attributed to either slight inaccuracies in the delineation of the entrapped phase structure, or to neglected physics (primarily, details of flow near the curved phase-phase interfaces), or both. On average, our algorithms for measurement of phase geometry place the interface at the outside edge of the entrapped nonwetting phase (see figure 1). Thus, we ignore flow in

the small curved wedges next to the phase interface. Compensating for this, transfer of shear between the fluids along the three-dimensional interface is also neglected. While these effects seem to be small for the current data set, additional analysis will be required in order to fully evaluate their influence.

Results (table 1) show that for the current experiments, τ is the dominant factor in determining k_{rs}, with S_f of second importance, followed by mean aperture within the flowing phase [(4) part A], and the effects of aperture distribution [(4) part B]. We also find that most of the parameters in (4) vary systematically with saturation (figure 3). The effects of aperture distribution [(4) part B] on k_{rs} are negligible, and hence can be ignored; the square of the mean aperture ratio appears to scale with $S_f^{0.4}$, and the tortuosity factor shows an approximate relationship with S_f^2. Inserting these approximations into (4) gives $S_f^{3.4}$, which is in reasonable agreement with the experimental estimates of k_{rs}, but not as good as those obtained from (4) with full knowledge of the parameters (table 1).

Finally, Nicholl et al. [1999] observed that the Reynolds equation overpredicted saturated transmissivity by 22-34% in aperture fields similar to those considered here. They concluded that depth averaging of pressure variation across the local aperture (b) did not fully account for three-dimensional flow induced by point-to-point aperture variation, Both our conceptual model, and full numerical simulations are depth averaged, yet yield predictions of k_r close to the experimental estimates. Apparently, inaccuracies resulting from depth averaging are similar in the saturated and satiated cases, and cancel out to a large extent for k_{rs}. This result is similar to that found for porous media, where k_r can be modeled well with simple conceptual models that neglect the details of the three-dimensional flow field within the pore network, while k is much less accurately predicted.

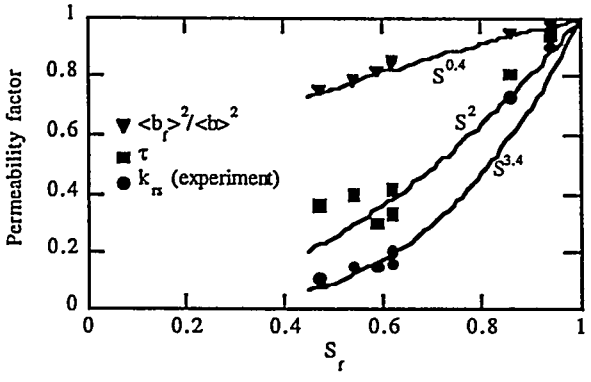

Figure 3. Factors contributing to relative permeability at satiation (krs) are shown as a function of flowing phase saturation (Sf). Combining the significant factors in (1) yields the S3.4 relation for krs.

Concluding remarks

We find close agreement between our simple conceptual model, numerical simulations, and experimental measurements. In-plane tortuosity (τ) is found to be the dominant factor controlling satiated relative permeability (k_{rs}). We also find that behavior across a wide range of phase structures can be approximated by a simple power law ($k_{rs} \approx S_f^n$). While the exponent arrived at here ($n \sim 3.4$) is no doubt specific to our experimental fracture, the fact that such a relationship exists, is in itself significant. In lieu of experimental studies across the range of possible fractures, rigorous models of the fluid invasion process can serve as a basis for estimating k_{rs} as a function of S_f. For instance, relationships between S_f at satiation, fluid properties, and aperture field statistics, such as those derived by Glass et al. [1998] in horizontal fractures, could be combined to yield estimates of k_{rs} for a significant range of conditions.

Acknowledgments. This work was supported by the U.S. Department of Energy's Basic Energy Sciences Geoscience Research Program under contract numbers DE-FG03-99ER14944 (Oklahoma State University), DE-FG03-96ER14590 (University of Colorado at Boulder), and DE-AC04-94AL85000 (Sandia National Laboratories). We also thank the two anonymous reviewers for their constructive comments.

References

Detwiler, R. L., S. E. Pringle, and R. J. Glass, Measurement of fracture aperture fields using transmitted light: An evaluation of measurement errors and their influence on simulations of flow and transport through a single fracture, *Water Resour. Res.*, 35(9), 2605-17, 1999.

Glass, R.J., M.J. Nicholl, and V.C. Tidwell, Challenging models for flow in unsaturated, fractured rock through exploration of small scale flow processes, *Geophysical Res. Letters*, 22(11), 1457-60, 1995.

Glass, R.J., M.J. Nicholl, and L. Yarrington, A modified invasion percolation model for low capillary number immiscible displacements in horizontal rough walled fractures: Influence of local in-plane curvature, *Water Resour. Res.*, 34(12), 3215-34, 1998.

Landau, L.D., and Lifshitz, *Electrodynamics of continuous media*, Pergamon Press, New York, 417 pp., 1960.

Nicholl, M.J., and R.J. Glass, Wetting phase permeability in a partially saturated horizontal fracture, *Proc. 5th Ann. Int. Conf. on High Level Rad. Waste Mgmt.*, 2007-19, American Nuclear Society, Las Vegas, Nevada, May 22-26, 1994.

Nicholl, M.J., H. Rajaram, R.J. Glass, and R. Detwiler, Saturated flow in a single fracture: Evaluation of the Reynolds Equation in measured aperture fields, *Water Resour. Res.*, 35(11), 3361-73, 1999.

Zimmerman, R.W., and G.S. Bodvarsson, Hydraulic conductivity of rock fractures, *Transport in Porous Media*, 23, 1-30, 1996.

M.J. Nicholl, School of Geology, Oklahoma State University, Stillwater, OK 74078. (e-mail: nicholl@okway.okstate.edu)

H. Rajaram, Department of Civil, Environmental, and Architectural Engineering, University of Colorado, Boulder, CO 80309-0428. (e-mail: hari@colorado.edu)

R.J. Glass, Flow Visualization and Processes Laboratory, Sandia National Laboratories, Albuquerque, NM 87185-1345. (e-mail: rjglass@sandia.gov)